Skeletal isomerization of 1-butene on synthetic clinoptilolite zeolite

Gon Seo [a,*], Myung-Wan Kim [a], Jong-Ho Kim [a], Byung Joon Ahn [b], Suk Bong Hong [c] and Young Sun Uh [c]

[a] *Department of Chemical Technology, Chonnam National University, Kwangju 500-757, Korea*
[b] *School of Chemical Science and Technology, Chonbuk National University, Chonju 561-756, Korea*
[c] *Korea Institute of Science and Technology, PO Box 131, Cheongryang, Seoul 130-650, Korea*

Received 1 June 1998; accepted 4 September 1998

A pure, highly crystalline clinoptilolite (CLI) zeolite with a Si/Al ratio of 5.8 has been synthesized using a small amount (1%) of seed crystals and tested as a catalyst for the skeletal isomerization of 1-butene at 623–723 K at atmospheric pressure. The catalytic results are compared to those obtained from a ferrierite (FER) zeolite with a Si/Al ratio of 7.6. It is found that selectivity for isobutene is very high on CLI zeolite, but conversion was lower than for FER zeolite. The simulated distribution and calculated potential profile of 1-butene molecules in CLI zeolite pore 10-ring channels show that the spatial constraints imposed by the pores are very severe. The exceptional selectivity and the low conversion of CLI zeolite results from the strict restriction of adsorption to very specific sites, inhibiting dimerization, as well as from the high potential barrier which reduces mass transfer.

Keywords: 1-butene skeletal isomerization, synthetic clinoptilolite, carbonaceous deposits, spatial constraints

1. Introduction

There are many examples where innovation in heterogeneous catalysis has been largely driven by industrial applications of zeolites and molecular sieves as shape-selective catalysts [1]. One recent example is the successful commercialization of a new catalytic process for the skeletal isomerization of linear butenes to isobutene based on the medium-pore zeolite ferrierite (FER) that contains a two-dimensional channel system consisting of 10-rings (4.2×5.4 Å) intersected by 8-rings (3.5×4.8 Å) [2,3].

Isobutene is a key component in the synthesis of methyl *tert*-butyl ether (MTBE), which is under growing demand as an ideal octane booster for gasoline. Thus, its availability has been a limiting factor in expanding the production of MTBE. This has led to a renewed interest in the skeletal isomerization of n-butenes, abundant feedstocks in actual refinery schemes, as the most promising way to increase the availability of isobutene [4]. To date, a wide variety of solid acids including halogenated alumina, zeolites, and phosphate-based molecular sieves have been studied as potential catalysts for this isomerization reaction [2–16]. Among these solid acids, FER zeolite is considered the best catalyst. As has been repeatedly shown in the literature [3,8], however, FER zeolite does not exhibit high selectivity for isobutene at the beginning of the skeletal isomerization of n-butenes due to the heavy formation of by-products (mainly propene and pentenes) via the extensive dimerization of n-butenes followed by cracking. The high selectivity for isobutene together with fairly good stability is obtained only after partial deactivation by carbonaceous deposits, i.e., coke. Thus, the initial isomerization selectivity of FER zeolite is much lower than that of other medium-pore materials such as ZSM-23 (MTT), SAPO-11 (AEL), and SAPO-41 (AFO), which possess a one-dimensional 10-ring channel system [13]. This implies that the pore structure of FER zeolite is not optimal for selectively isomerizing n-butenes to isobutene, although it plays a significant role in achieving high isomerization selectivity. Apparently, pore size in zeolites and related materials is crucial for the skeletal isomerization of n-butenes since all of the microporous materials which are succesful for this isomerization have 10-ring molecular sieves. The pore openings on 8-ring zeolites are too small to allow the free transport of isobutene. 12-ring materials do not possess the shape selectivity to effectively suppress side reactions, such as n-butene dimerization followed by cracking to light hydrocarbons. Therefore, the first step in finding a catalyst which is ideally suited to steer the isomerization of n-butenes towards the skeletal isomer rather than dimerization products should be the continuous testing of new 10-ring microporous materials.

Clinoptilolite is one of the most abundant natural zeolites and is isostructural with the zeolite heulandite [17]. Thus, it contains a two-dimensional pore system consisting of 8-ring channels (2.6×4.7 Å) that intersect two parallel 10-ring channels (3.0×7.6 Å) and 8-ring channels (3.3×4.6 Å) [18]. This natural zeolite has been found suitable for many potential applications in ion exchange, gas separation, and catalysis [19–23]. In particular, a recent study by Woo et al. [24] has shown that natural clinoptilolite is an effective catalyst for the skeletal isomerization of 1-butene to isobutene. However, extensive investigations of its physicochemical and catalytic properties are limited by the presence of relatively large amounts of iron impurities, α-quartz, and/or other zeolitic phases that are difficult

* To whom correspondence should be addressed.

to remove completely from the zeolite. Therefore, much interest has been directed toward the hydrothermal synthesis of clinoptilolite using an alkali-metal aluminosilicate gel, as a starting phase. Numerous papers on this topic have been published [25–31] demonstrating that clinoptilolite can be hydrothermally synthesized, both with and without seed crystals present, although the crystallization conditions and the composition of reaction mixtures leading to successful clinoptilolite formation are restricted within narrow limits. In contrast to the volume of work on the synthesis of this zeolite, however, no investigations involving the utilization of synthetic clinoptilolite as a separation medium or as a catalyst have yet been reported. In this study, we synthesized a pure clinoptilolite with a Si/Al ratio of 5.8 using a seeding technique, investigated its catalytic performance for the skeletal isomerization of 1-butene under various operating conditions, and compared the catalytic results to those obtained from a FER zeolite with a Si/Al ratio of 7.6. In addition, the influence of coke deposits on the activity and selectivity of synthetic clinoptilolite is discussed.

2. Experimental

2.1. Samples

A clinoptilolite zeolite with a Si/Al ratio of 5.8 was synthesized using a seeding technique following a procedure described in the literature [30,31]. In a typical synthesis, 3.22 g aluminum hydroxide hydrate ($Al(OH)_3{\cdot}0.5H_2O$, Aldrich) was dissolved in a clear solution obtained by combining 1.98 g NaOH (50% aqueous solution, Aldrich), 13.56 g KOH (45% aqueous solution, Aldrich), and 32.35 g of deionized water. After stirring this solution for 0.5 h, 50.0 g of aqueous colloidal silica (Ludox AS-40, DuPont) were added. The gel composition of the resulting mixture was $1.67Na_2O{\cdot}7.34K_2O{\cdot}2.5Al_2O_3{\cdot}45SiO_2{\cdot}550H_2O$. To this reaction mixture, 0.34 g (1 wt% of anhydrous raw materials) of seed crystals were added. The seed crystals used here were synthetic clinoptilolite, which was previously prepared by using natural clinoptilolite (Youngil, Korea) as a seed, following the method stated above. The final reaction mixture was stirred at room temperature for 48 h, sealed in a teflon-lined autoclave and heated at 423 K, without stirring under autogenous pressure, for 8 days. The solid product was recovered by filtration, washed repeatedly with distilled water, and then dried overnight at room temperature. As-synthesized clinoptilolite was refluxed twice in 1.0 NH_4NO_3 solution and then calcined in air at 773 K for 16 h in order to obtain the acid form. Here we denote the as-synthesized clinoptilolite and its acid form as NaK-CLI and H-CLI, respectively. For comparison, a FER zeolite having a Si/Al ratio of 7.6 was prepared and converted to the acid form (H-FER) according to procedures described elsewhere [15].

2.2. Analysis

The X-ray diffraction patterns of the zeolites thus prepared were recorded on a Rigaku D/Max-IIIA diffractometer using Kα radiation. Chemical analysis was performed by a Jarrell-Ash Polyscan 61E inductively coupled plasma (ICP) spectrometer. The nitrogen BET surface areas were measured on a house-built volumetric adsorption unit. Adsorption of n-hexane on CLI and FER zeolites was examined by a quartz-spring balance at 298 K to compare the spatial constraints of their pores. The acidic properties of the zeolites were determined by the temperature-programmed desorption (TPD) of ammonia using a TPD apparatus described previously [15]. Thermogravimetric analyses of the zeolite catalysts after the skeletal isomerization of 1-butene were carried out on a DuPont 950 thermogravimetric analyzer, where weight loss related to the combustion of deposited coke was determined from differential thermal analyses (DTA) using a Shimadzu differential thermal analyzer [16]. Approximately 20 mg of sample was heated in air to 1073 K with a ramping rate of 5 K min^{-1}. The color of all zeolite samples changed from dark gray or black to white after thermal analyses, indicating that the weight loss attributable to the combination of TGA and DTA can be regarded as a measure of the coke deposited on the catalyst.

The preferred locations of 1-butene and isobutene molecules on CLI and FER zeolites were determined by Monte Carlo simulation and energy minimization techniques. The Burchart-Universal force field implemented in the Cerius^2 sorption software was used for both the docking and energy minimization calculations [32]. These calculations were performed using $2 \times 2 \times 3$ unit cells of CLI and FER zeolites with an additional 6.6 Å shell of structure surrounding them, and iterated 10^6 times to obtain a clear distribution file. The zeolite framework was held fixed during the simulation, while sorbates were mobile. The change in the potential energy of 1-butene molecules in the CLI and FER zeolites 10-ring channels was also calculated. 1-butene molecule moved by 0.1–0.2 Å along the channel, and the lowest energy was determined.

2.3. Catalysis

A conventional continuous flow microreactor was used to conduct the skeletal isomerization of 1-butene over zeolite catalysts at atmospheric pressure. A reactant stream with an Ar/1-butene molar ratio of 0.3–5.3 was fed into a stainless steel reactor containing the catalyst at the desired reaction temperature, in order to study the influence of the partial pressure of 1-butene on isomerization. The catalyst was activated under flowing Ar (50 cm^3 min^{-1}) at 673 K for 1 h before the feed was introduced, and the 1-butene velocity, WHSV, was fixed at 3.0 h^{-1}. The reaction products were analyzed on-line in a Varian 1420 gas chromatograph equipped with a sebaconnitrile column and a thermal conductivity detector, with the first analysis carried out after

10 min on stream. The conversion of 1-butene was calculated on the hypothesis that the three n-butene isomers (i.e., 1-butene, *cis*-2-butene, and *trans*-2-butene) were acting as reactants. Selectivity for isobutene was calculated by dividing the isobutene yield by the 1-butene conversion.

3. Results and discussion

3.1. Physicochemical properties of synthetic clinoptilolite

Figure 1 shows the X-ray diffraction patterns of NaK-CLI and H-CLI zeolites, i.e., the as-synthesized and acid forms of CLI zeolite prepared in this study. All reflection from NaK-CLI zeolite was understood to arise from a zeolite with a heulandite structure, indicating that it is of pure phase. The chemical composition data given in table 1 reveal that NaK-CLI zeolite has a Si/Al ratio > 4 and contains no Ca^{2+} ions, within experimental error. Therefore, this sample must be referred as clinoptilolite rather than as heulandite. Table 1 also shows that the K^+ ion is highly enriched in the NaK-CLI sample, which is consistent with the trend found in typical syntheses of heulandite-type zeolites in the literature [28–30]. As seen in figure 1, on the other hand, the X-ray diffraction pattern of H-CLI zeolite is essentially identical with that of NaK-CLI zeolite except that the relative peak intensities are somewhat different. This clearly shows that CLI zeolite prepared here maintains its structural integrity during the NH_4^+ ion exchange and calcination step. Further evidence to support the above speculation can be obtained from the nitrogen BET surface area measurements. As shown in table 1, the BET surface area of H-CLI zeolite was found to be 386 $m^2\,g^{-1}$, revealing that this sample is highly crystalline. In contrast, NaK-CLI zeolite exhibited a surface area of only 11 $m^2\,g^{-1}$. This is most likely due to the steric effects caused by the blocking action of inorganic cations (mainly K^+ ions) present in the inner pores of the NaK-CLI zeolite. The fact that nitrogen is not adsorbed in the pore of NaK-CLI zeolite indicates that the spatial constraints of CLI zeolite are more severe than those of FER zeolite, although the main channels for both zeolites are 10-ring channels.

Figure 2 shows the results of the ammonia TPD obtained from the H-CLI and H-FER zeolites that are used as catalysts for the skeletal isomerization of 1-butene in this study. Both TPD curves in figure 2 are characterized by two desorption peaks with maxima in the temperature

Table 1
Physical properties of zeolites used in this study.

Sample	Structure type	Anhydrous unit cell composition	Si/Al ratio	BET surface area[a] ($m^2\,g^{-1}$)
NaK-CLI	HEU	$Na_{0.1}K_{5.2}Al_{5.3}Si_{30.7}O_{72}$	5.8	11
H-CLI	HEU	$H_{5.3}Al_{5.3}Si_{30.7}O_{72}$	5.8	386
H-FER	FER	$H_{4.2}Al_{4.2}Si_{31.8}O_{72}$	7.6	364

[a] BET surface areas calculated from nitrogen adsorption data.

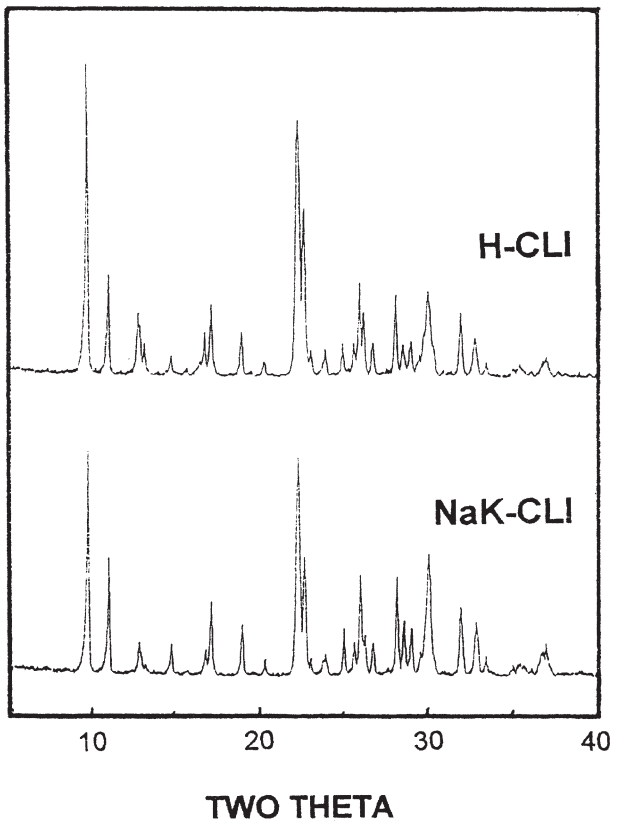

Figure 1. X-ray powder diffraction patterns of (a) NaK-CLI and (b) H-CLI zeolites.

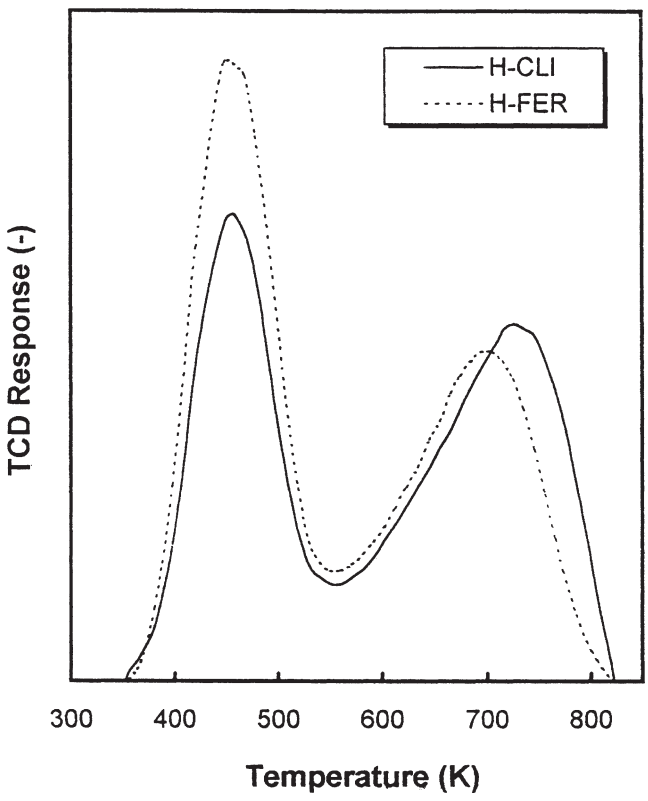

Figure 2. Ammonia TPD profiles from (a) H-CLI and (b) H-FER zeolite catalysts.

regions of 460–480 and 680–730 K, which correspond to weak and strong acid sites, respectively. Total areas of ammonia desorption from H-CLI and H-FER zeolites are similar to each other. The temperature maximum of the second desorption peak from the H-CLI zeolite is slightly higher than that from the H-FER zeolite. The difference in the temperature maxima may be due to acidic strength. Otherwise, the readsorption of ammonia during TPD shifts maximum temperature higher for zeolites with a great number of acid sites [33]. It is well known that acidity and pore size are the two important parameters affecting the activity and selectivity of zeolites and related materials during 1-butene skeletal isomerization [34,35]. However, the fact that the difference is not large, as shown in figure 2, reveals that the H-CLI and H-FER zeolites prepared for this study have similar acidic properties. Therefore, the catalytic results obtained from these two zeolites should illustrate the effects of the geometrical constraints imposed by the particular pore structure of the catalysts.

3.2. Catalytic isomerization of 1-butene

Table 2 lists the conversions and product distributions from the skeletal isomerization of 1-butene on H-CLI and H-FER zeolites measured at 623–723 K, 3.0 h^{-1} WHSV, 31 kPa 1-butene pressure in the feed and 70 min time on stream. The most appropriate way to compare different zeolite catalysts is to examine their isomerization selectivity at nearly the same level of conversion, since the selectivity of microporous materials for isobutene differs significantly according to the 1-butene conversion [3,12,13]. Table 2 shows that at 623 K and conversion levels near 15%, the selectivity for isobutene was 74.6 and 58.5% for H-CLI and H-FER catalysts, respectively. It was also observed that the H-CLI catalyst produces a smaller amount of propene and pentenes compared to the H-FER catalyst. Due to the presence of a high concentration of reactants inside the zeolite pores, dimerization of 1-butene molecules is a serious competing reaction where the dimerized products (octenes) are further cracked into two major by-products, namely propene and pentenes. Obviously, the excellent performance of the 10-ring medium-pore molecular sieves for the skeletal isomerization of 1-butene comes from their shape selectivity, so that they can suppress undesired bimolecular processes for which large spaces are required. However, the extent of suppression is greatly influenced by the shape of the 10-ring pores, as well as by their size [13]. Recall that the 10-ring channels (3.0×7.6 Å) of H-CLI zeolite are much more elliptical than those (4.2×5.4 Å) of H-FER zeolite despite the similarity in pore dimension. This suggests that the spatial constraints suppressing 1-butene dimerization inside the 10-ring channels may be higher for H-CLI zeolite than for H-FER zeolite. Therefore, we speculate that the reason the H-CLI catalyst is more selective for isobutene formation than the H-FER catalyst is that the oval-shaped H-CLI 10-ring channels are too narrow for bimolecular transformation of 1-butene.

Table 2
Conversion and product distribution from 1-butene skeletal isomerization on H-CLI and H-FER zeolites at different temperatures.[a]

Catalyst	Reaction temp. (K)	Conversion (%)	Selectivity (%)					
			$C_2^=$	C_3	$C_3^=$	n-C_4	i-$C_4^=$	C_{5+}
H-CLI	623	15.9	0.4	0.0	10.0	6.1	74.6	8.8
	673	16.1	0.0	3.5	7.0	5.4	80.7	3.4
	723	16.0	0.0	0.0	4.8	2.6	89.5	3.1
H-FER	623	16.5	0.0	1.9	18.5	7.9	58.5	13.2
	673	33.1	0.6	1.0	10.6	3.4	74.2	10.2
	723	38.1	0.9	0.3	9.1	10.5	71.6	7.6

[a] Data are reported as the average values of 70 min time on stream at WHSV = 3.0 h^{-1}.

Another interesting observation obtained from table 2 is that the selectivity of the H-CLI catalyst for isobutene was enhanced by elevating the reaction temperature, while the degree of 1-butene conversion remained almost unchanged. This trend exists at least over the temperature range studied here and suggests that the highly elliptical 10-ring channels of H-CLI zeolite do not allow the free diffusion of isobutene. Table 2 also shows that selectivities for propene and pentenes, which must be produced through the dimerization–cracking process, are continuously decreased on both H-CLI and H-FER catalysts at higher reaction temperatures. This is not surprising because 1-butene dimerization becomes thermodynamically unfavored at high temperatures [11]. As stated earlier, however, the selectivity of the H-CLI catalyst for isobutene increases while cracking decreases. Therefore, it is most likely that the skeletal isomerization of 1-butene to isobutene on H-CLI proceeds through a monomolecular mechanism rather than a bimolecular mechanism, in the same fashion as for the H-FER catalyst [9,13–16].

Figure 3 shows 1-butene conversion and selectivity for isobutene as a function of time on stream in skeletal isomerization over H-CLI and H-FER zeolites at 723 K, 3.0 h^{-1} WHSV, and 31 kPa 1-butene in the feed. For an initial 10 min time on stream, 1-butene dimerization followed by cracking to light olefins was found to be a very serious side reaction that may decrease the selectivity for isobutene. As time on stream increases, however, these bimolecular processes are significantly suppressed. Thus, 1-butene conversion decreases with increasing time on stream. In particular, sharp decreases in 1-butene conversion are observed at early times on stream. In contrast, the selectivity for isobutene increases rapidly at 70 min time on stream and remains almost unchanged over the period of time studied. These results have also been observed during 1-butene isomerization on other 10-ring medium-pore materials such as TON and MTT zeolites [8,9]. It is well established that the origin of a remarkable increase in selectivity for isobutene of these 10-ring zeolites with time on stream is coke formation inside the zeolite channels, which would reduce the free space around the acid sites and thus suppress the dimerization reactions. In addition, poisoning of the exterior acid sites by coke deposition may contribute to the

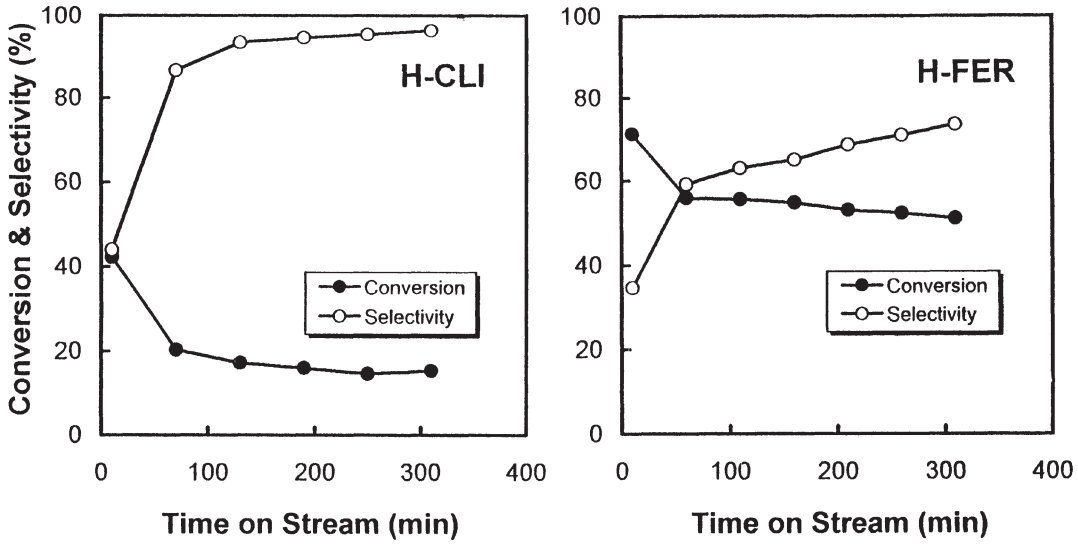

Figure 3. 1-butene conversion and selectivity for isobutene as a function of time on stream in skeletal isomerization over H-CLI and H-FER [15] zeolites at 723 K, 3.0 h^{-1} WHSV, and 31 kPa 1-butene pressure.

increased isobutene selectivity since they favor dimerization over isomerization. On the basis of these speculations therefore, one can explain why fresh H-CLI zeolite produces a large amount of by-products in the beginning of the reaction and becomes more selective for isobutene formation only after a certain period of induction time. The drastic change in the conversion and the selectivity of the H-CLI catalyst suggests that the spatial constraint of H-CLI zeolite is more severe than that of H-FER zeolite, resulting in the higher selectivity and lower conversion.

Figure 4 shows coke formation for the fresh H-CLI catalyst during the skeletal isomerization of 1-butene at 723 K, 3.0 h^{-1} WHSV, and 31 kPa 1-butene pressure, as a function of time on stream. As seen in figure 4, coke formation on this zeolite is initially fast but slows down rapidly with time on stream. Thus, the level of coke deposited on the H-CLI catalyst during the 5 h on stream which we studied was found to be ∼7%. At this coke level, however, the H-CLI catalyst was highly active and selective for the skeletal isomerization of 1-butene (see figure 3). This clearly shows that the high isomerization selectivity of the H-CLI catalyst can be achieved only after partial deactivation by coke, which is consistent with the trend found in the H-FER catalyst [3,36]. Most likely, the increased spatial constraints by coke deposition limiting n-butene dimerization may be responsible for the enhancement of selectivity for isobutene. Also, it should be noted that the level (7%) of the coke formed in H-CLI catalyst is slightly lower than that (8–10%) of properly used H-FER catalyst, producing high isobutene selectivity [3,36]. This can be rationalized by considering that the 10-ring pores of H-CLI zeolite are much narrower than those of H-FER zeolite.

Figure 5 shows plots of 1-butene conversion and isobutene selectivity on the H-CLI catalyst versus partial pressure of 1-butene. Both 1-butene conversion and selectivity for isobutene were found to decrease with increased partial pressure of 1-butene. Thus, the highest degree of

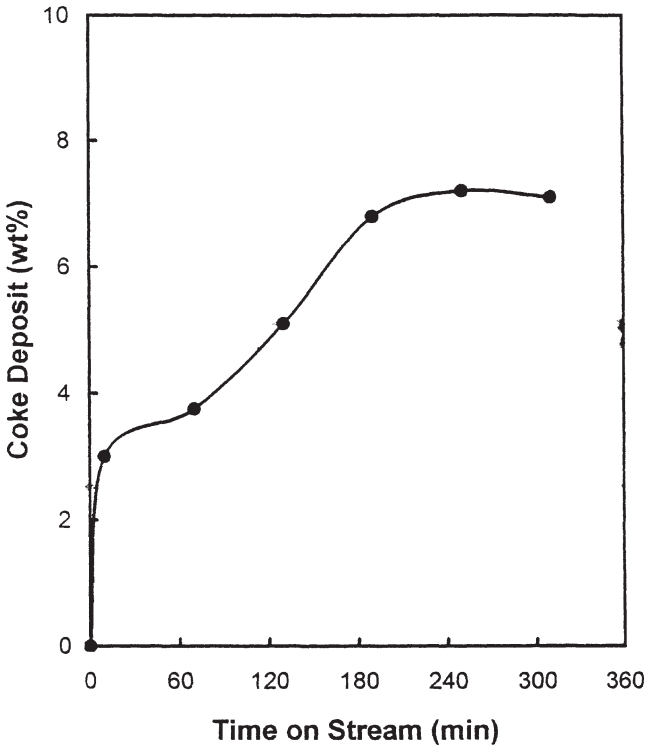

Figure 4. Coke formation for fresh H-CLI zeolite during the skeletal isomerization of 1-butene at 723 K, 3.0 h^{-1} WHSV, and 31 kPa 1-butene pressure as a function of time on stream.

1-butene conversion and the best selectivity for isobutene was achieved at the lowest partial pressure of 1-butene in the pressure range studied here. In particular, selectivity for isobutene decreases sharply when the partial pressure of 1-butene in the feed is 90 kPa. This result does not accord with the catalytic results for H-FER reported previously [15]. Since dimerization reaction is accelerated with increased 1-butene pressure, it is natural that conversion increases and selectivity decreases with increasing partial

pressure. Therefore, the sharp decrease of conversion over the H-CLI catalyst at high 1-butene pressure is due to pore blocking by coke deposition. Since the entrance of CLI zeolite pore is narrow, ion exchanges of alkali metal ions to protons are required for the adsorption of nitrogen. This means that even a small amount of carbon deposited on the external surface hampers the diffusion of reactant into the pores, resulting in very low conversion.

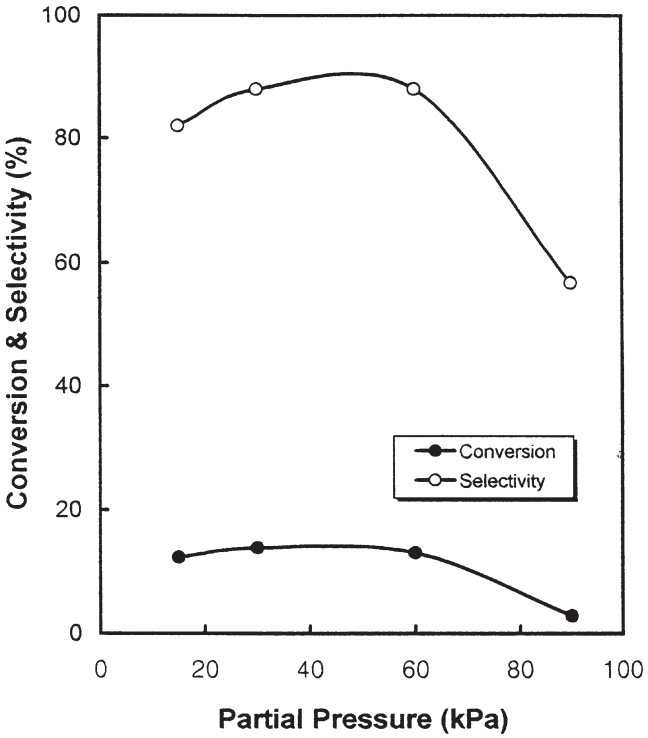

Figure 5. 1-butene conversion and selectivity for isobutene as a function of partial pressure of 1-butene in skeletal isomerization over H-CLI catalyst at 723 K, 3.0 h^{-1} WHSV, and 130 min time on stream.

Although the sorption simulation results of reactant and/or product guest molecules in zeolites are somewhat altered according to the force field and the calculation method used, they can provide valuable information about the spatial location and dynamic behavior of adsorbed molecules which are difficult to ascertain by experimental methods [32,37]. Figure 6 shows the simulated distributions of 1-butene molecules adsorbed at 300 K and 100 kPa on CLI and FER zeolites. A recent simulation study on the butene isomers in H-FER zeolite with a Si/Al ratio of 8 have revealed that coulombic interactions have almost no influence on the diffusion properties [37]. Thus, our calculations were restricted to the pure-silica framework. The distribution probability of the preferred locations of these two butene isomers was obtained from 10^6 iterated calculations and each center of mass of adsorbed molecules was indicated by a dot for clarity. Figure 6 clearly shows that 1-butene molecules are mainly located in the intersections of 10- and 8-ring channels of CLI and FER zeolites, and are thus far apart from each other. Therefore, it is most likely that the collision probability between the molecules adsorbed on CLI and FER zeolites may be low enough to suppress side reactions such as the dimerization of 1-butene followed by cracking to propene and pentenes.

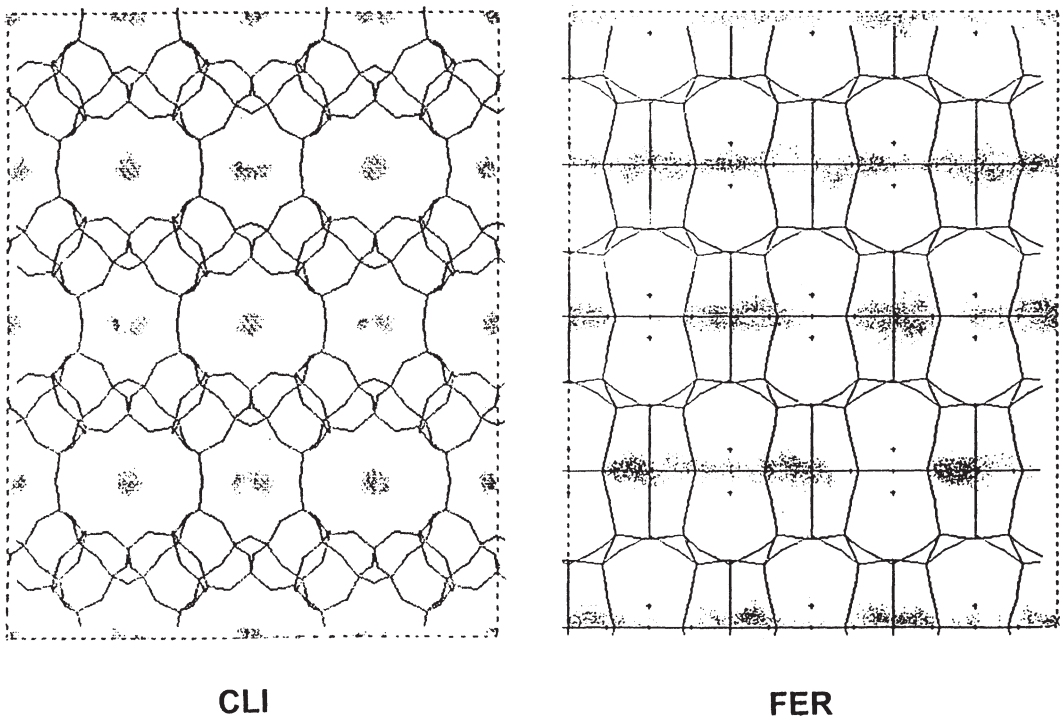

Figure 6. Simulation results of 1-butene molecules adsorbed at 300 K and 100 kPa on pure-silica CLI and FER [32] zeolites. The presented structure covers $2 \times 2 \times 3$ unit cells along [001]. For clarity, each center of mass of adsorbed molecules is indicated by a dot.

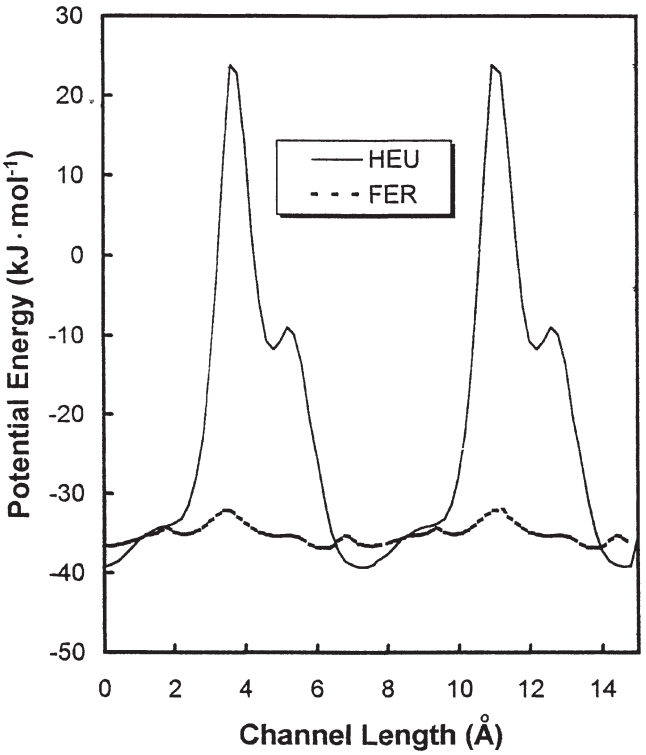

Figure 7. Potential energy profiles of 1-butene molecule moving in 10-ring channels of pure-silica CLI and FER zeolites at 300 K and 100 kPa.

The concentrations of dots denoting 1-butene molecules on CLI zeolite pores differ notably from those on FER zeolite. The dots on CLI zeolite make small circles, while the dots on FER zeolite are dispersed in intersections forming ellipses. This means the preferable position of 1-butene in a CLI zeolite is very specific, while 1-butene molecules in FER zeolite are dispersed in the pore with more freedom. This result can be confirmed by calculated potential energy profiles for 1-butene molecules on CLI and FER zeolites, as shown in figure 7. The extremely high potential barrier for the movement of 1-butene molecules in the CLI zeolite 10-ring channels indicates that there is a specific position where the 1-butene molecule must be located. Although there is also a potential barrier for FER zeolite, it is very small compared to that of CLI zeolite. The low potential barrier for FER zeolite can also be surmised from the dispersed distribution of 1-butene (figure 6) and the relatively low selectivity for isobutene (figure 3) compared with CLI zeolite.

The high potential barrier in CLI zeolite results in the slow diffusion of the reactant as well as the specific distribution of molecules in the pore. n-hexane was adsorbed on H-FER zeolite very fast at 303 K and the adsorption amount reached 0.14 g/g zeolite at 30 min under a 1-butene pressure of 30 kPa. By contrast, no meaningful uptake of n-hexane on the H-CLI zeolite was observed until 30 min. This clearly shows that there is a high spatial constraint in CLI zeolite pores for 1-butene molecule. This suggests that the extent of suppression of 1-butene bimolecular processes is more strict for H-CLI zeolite than for H-FER zeolite, which may be responsible for its high selectivity for isobutene and low conversion.

In conclusion, the catalytic results presented in this study demonstrate that synthetic CLI zeolite is a highly selective catalyst for the skeletal isomerization of 1-butene to isobutene. It was found that at nearly the same level of conversion, selectivity for 1-butene is higher for CLI zeolite than for FER zeolite with the major difference being that CLI zeolite produces smaller amounts of cracked products (mainly propene and pentenes). In addition, synthetic CLI zeolite shows a noticeable increase in isobutene selectivity within a very short reaction time, which can be attributed to the masking of acid sites on the external surface and the increased spatial constraints inside the pores by coke deposition that restrict undesired side reactions, especially the dimerization–cracking process. The potential energy profile of 1-butene molecules in CLI zeolite pores shows that there is a large potential difference along the 10-ring channel. Thus, the preferable sites for 1-butene molecules adsorbed in the pores are very specific, and they are held far enough apart from each other to decrease the possibility of dimerization. Since the spatial constraint CLI zeolite pores impose on 1-butene is exceptional, the selectivity for isobutene is exceptional, but the conversion is low due to the slower diffusion restricted by the high potential barrier. Although the low potential barrier of 1-butene molecules in FER zeolite is responsible for the lower selectivity compared to that in CLI zeolite, it is most likely that the main reason FER zeolite is used as an industrial catalyst for the skeletal isomerization of n-butenes is the fast mass transfer of reactants in the pores of this zeolite, giving a high yield of isobutene.

Acknowledgement

This work was supported by the Korea Science and Engineering Foundation (971-1108-052-2) and the Korea Institute of Science and Technology. One (SBH) of the authors thanks Dr. K. Itabashi of Tosoh Corporation for helpful discussions, and Professor L. Kevan of the Chemistry Department at the University of Houston for sending a preprint of his work.

References

[1] J.M. Thomas and W.J. Thomas, *Principles and Practice of Heterogeneous Catalysis* (VCH, Weinheim, 1997).
[2] P.B. Grandvallet, K.P. de Jong, H.H. Mooiweer, A.G.T. Kortbeek and B. Kraushaar-Czarnetzki, Eur. Patent 501, 577 (1992).
[3] H.H. Mooiweer, K.P. de Jong, B. Kraushaar-Czarnetzki, B.W.H. Stork and B.C.H. Krutzen, Stud. Surf. Sci. Catal. 84 (1994) 2327.
[4] A.C. Butler and C.P. Nicolaides, Catal. Today 18 (1993) 443.
[5] J. Szabo, J. Perrotey, G. Szabo, J.C. Duchet and D. Cornet, J. Mol. Catal. 67 (1991) 79.
[6] G. Seo, N.-H. Kim, Y.-H. Lee and J.-H. Kim, Catal. Lett. 51 (1998) 101.
[7] W.-Q. Xu, Y.-G. Yin, S.L. Suib, J.C. Edwards and C.-L. O'Young, J. Catal. 150 (1994) 34.

[8] W.-Q. Xu, Y.-G. Yin, S.L. Suib, J.C. Edwards and C.-L. O'Young, J. Phys. Chem. 99 (1995) 9443.
[9] C.-L. O'Young, R.J. Pellet, D.G. Casey, J.R. Ugolini and R.A. Sawicki, J. Catal. 151 (1995) 467.
[10] L.H. Gielgens, I.H.E. Veenstra, V. Ponec, M.J. Haanepen and J.H.C. van Hooff, Catal. Lett. 32 (1995) 195.
[11] J. Houzvicka, O. Diefenbach and V. Ponec, J. Catal. 164 (1996) 288.
[12] M. Guisnet, P. Andy, N.S. Gnep, E. Benazzi and C. Travers, J. Catal. 158 (1996) 551.
[13] P. Meriaudeau, V.A. Tuan, N.H. Le and G. Szabo, Catal. Lett. 47 (1997) 71.
[14] P. Meriaudeau, V.A. Tuan, N.H. Le and G. Szabo, J. Catal. 169 (1997) 397.
[15] G. Seo, H.S. Jeong, S.B. Hong and Y.S. Uh, Catal. Lett. 36 (1996) 249.
[16] G. Seo, H.S. Jeong, D.-L. Jang, D.L. Cho and S.B. Hong, Catal. Lett. 41 (1996) 189.
[17] D.E.W. Vaughan, in: *Natural Zeolites; Occurrence, Properties, Uses*, eds. L.B. Sand and F.A. Mumpton (Pergamon, Oxford, 1978) p. 353.
[18] W.M. Meier, D.H. Olson and C. Baerlocher, *Atlas of Zeolite Structure Types* (Elsevier, New York, 1996).
[19] G. Gottardi and E. Galliey, *Natural Zeolites* (Springer, Heidelberg, 1985) p. 256.
[20] D. Leppert, Min. Eng. (Littleton Colo.) 42 (1990) 604.
[21] M.A. Ackley and R.T. Yang, Ind. Eng. Chem. Res. 30 (1991) 2523.
[22] R.W. Triebe and F.H. Tezel, Gas Sep. Purif. 9 (1995) 223.
[23] H. Sakoh, M. Nitta and K. Aomura, Appl. Catal. 16 (1985) 249.
[24] H.C. Woo, K.H. Lee and J.S. Lee, Appl. Catal. A 134 (1996) 147.
[25] L.L. Ames, Jr., Am. Mineral. 48 (1963) 1374.
[26] Y. Goto, Am. Mineral. 62 (1977) 330.
[27] D.B. Hawkins, R.A. Sheppard and A.J. Gude, in: *Natural Zeolites; Occurrence, Properties, Uses*, eds. L.B. Sand and F.A. Mumpton (Pergamon, Oxford, 1978) p. 337.
[28] C.-H. Chi and L.B. Sand, Nature 304 (1983) 255.
[29] R.N. Sanders and S.M. Laurent, US Patent 4,623,529 (1986).
[30] S. Satokawa and K. Itabashi, Micropor. Mater. 8 (1997) 49.
[31] D. Zhao, R. Szostak and L. Kevan, submitted.
[32] G. Seo, H.S. Jeong, J.M. Lee and B.J. Ahn, Stud. Surf. Sci. Catal. 105 (1997) 1431.
[33] J.L. Falconer and J.A. Schwarz, Catal. Rev. Sci. Eng. 25 (1983) 141.
[34] W.-Q. Xu, S.L. Suib and C.-L. O'Young, J. Catal. 144 (1993) 285.
[35] M.A. Asensi, A. Corma and A. Martinez, J. Catal. 158 (1996) 561.
[36] W.-Q. Xu, Y.-G. Yin, S.L. Suib and C.-L. O'Young, J. Phys. Chem. 99 (1995) 758.
[37] F. Jousse, L. Leherte and D.P. Vercauteren, Mol. Simul. 17 (1996) 175.